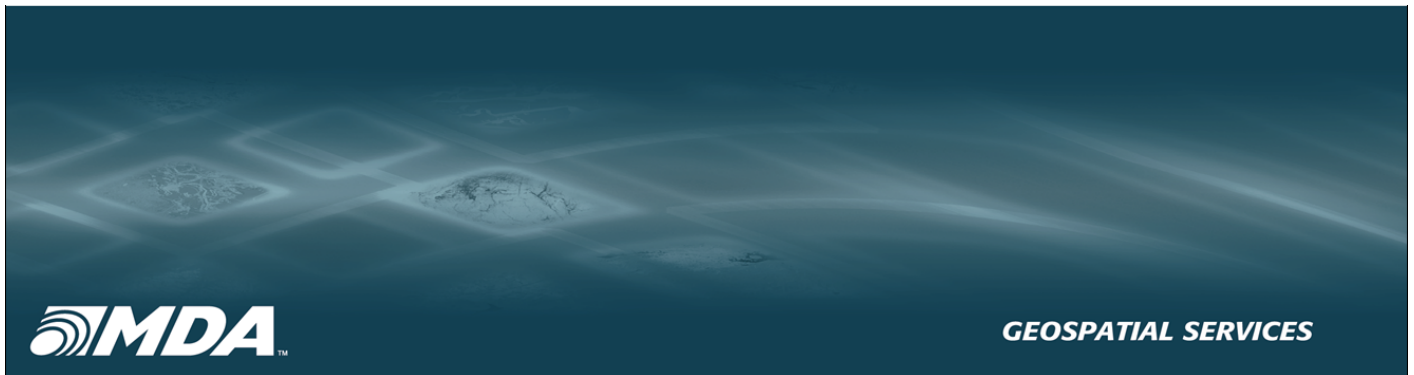


# Playa del Rey, California InSAR Ground Deformation Monitoring Interim Report B

Ref.: RV-14524  
January 15, 2010



SUBMITTED TO:

**Southern California Gas Company**  
555 W. Fifth Street (Mail Location 23E2)  
Los Angeles, CA, USA  
90013-1041

ATTN: Mr. Rick Gailing

SUBMITTED BY:

**MDA Geospatial Services**  
57 Auriga Drive, Suite 201  
Ottawa, Ontario K2E 8B2  
CANADA

Tel: +1-613-727-1087  
Fax: +1-613-727-5853

©MDA Geospatial Services Inc., 2010.

All Rights Reserved

### **Restriction on Use, Publication or Disclosure of Proprietary Information**

This document contains information proprietary to MDA Geospatial Services Inc. ("MDA GSI"), a wholly owned subsidiary of MacDONALD DETTWILER AND ASSOCIATES LTD., their subsidiaries, or a third party to which they may have a legal obligation to protect such information from unauthorized disclosure, use or duplication. Any disclosure, use or duplication of this document or of any of the information contained herein for other than the specific purposes for which it was disclosed is expressly prohibited, except as MDA GSI may have otherwise agreed to in writing.





Prepared By: \_\_\_\_\_ January 15, 2010  
Mary Anne McParland  
Remote Sensing Analyst

Reviewed By: \_\_\_\_\_ January 15, 2010  
Michael Henschel  
Sr. SAR Specialist





## Executive Summary

This report, Interim Report B, describes the results and methodology used to monitor as well as quantify potential ground deformation at the Southern California Gas Company (SoCalGas) Playa del Rey Gas Storage Field and surrounding areas in California using InSAR satellite radar interferometry for the June 2009 to December 2009 monitoring time period.

The RADARSAT-2 satellite passes over SoCalGas' Area of Interest (AOI) every 24 days at an elevation of approximately 500 miles. The acquired RADARSAT-2 imagery is being used for the generation of deformation maps over the AOI, two (2) of which are delivered to SoCalGas every 6 months. The accuracy of each deformation map is estimated to be in the order of 0.02 ft.

For this deliverable, Milestone 3, two (2) deformation products are produced from scheduled RADARSAT-2 Ultra-Fine ascending radar imagery. The current deformation data produced from June 15, 2009 to December 24, 2009 time period are reviewed as part of this Milestone.

The following summarizes key features for this deliverable:

- Satellite radar data were scheduled for acquisition from June 2009 through to December 2009. For this deliverable, nine (9) ascending RADARSAT-2 Ultra-Fine ascending radar data were collected and analyzed.
- All available data are evaluated and the highest quality deformation maps are generated. The time periods are from June 15, 2009 to September 19, 2009 (Pair A) and September 19, 2009 to December 24, 2009 (Pair B).
- The delivered products are geo-referenced with a horizontal accuracy better than 65 ft. Areas of insufficient quality are masked out in the final products. The measurements in the AOI are of good quality.
- The estimated precision for the pair June 15, 2009 to September 19, 2009 vertical deformation product is 0.019 ft with a 95% confidence interval; while the estimated precision for pair September 19, 2009 to December 24, 2009 vertical change product is 0.0148 ft with a 95% confidence interval.
- Two (2) summation products are generated. The first is for the six (6) month time period from June 15, 2009 to December 24, 2009 (Pair C). For this period, masked areas are interpolated and common mask areas between the two individual vertical deformation products are extracted and applied to the final summation product.



- The second summation product includes approximately one and a half (1.5) years of monitoring from May 27, 2008 to December 24, 2009 (Pair D). This was derived by combining the previous and current time period summation products. Mask areas for this overall summation is an accumulation of all the previous masks.



## Contents

<b>1 Interim Report B Objective</b>	<b>1</b>
1.1 Report Organization . . . . .	1
1.2 Study Area . . . . .	1
1.3 Data Selection . . . . .	3
<b>2 Results - Interim Report B</b>	<b>4</b>
2.1 Pair A - June 15, 2009 to September 19, 2009 . . . . .	5
2.2 Pair B - September 19, 2009 to December 24, 2009 . . . . .	9
2.3 Pair C - Summation June 15, 2009 to December 24, 2009 . . . . .	13
2.4 Pair D - Summation May 27, 2008 to December 24, 2009 . . . . .	19
<b>3 Concluding Remarks</b>	<b>26</b>
<b>A Deliverables</b>	<b>27</b>
<b>B Standard Definitions</b>	<b>28</b>



## List of Figures

1	Playa del Rey AOI and surrounding area in Los Angeles, as outlined by red polygon (radar amplitude image). . . . .	2
2	Zoom-in of Playa del Rey AOI. Colour representation of the vertical deformation product from June 15, 2009 to September 19, 2009 superimposed on SAR image without contours. . . . .	6
3	Zoom-in of Playa del Rey AOI. Colour representation of the vertical deformation product from June 15, 2009 to September 19, 2009 superimposed on SAR image with 0.01 ft contours. . . . .	7
4	Zoom-in of Playa del Rey Gas Storage Field. Colour representation of the vertical deformation product from June 15, 2009 to September 19, 2009 superimposed on SAR image with 0.01 ft contours. . . . .	8
5	Zoom-in of Playa del Rey AOI. Colour representation of the vertical deformation product from September 19, 2009 to December 24, 2009 superimposed on SAR image without contours. . . . .	10
6	Zoom-in of Playa del Rey AOI. Colour representation of the vertical deformation product from September 19, 2009 to December 24, 2009 superimposed on SAR image with 0.01 ft contours. . . . .	11
7	Zoom-in of Playa del Rey Gas Storage Field. Colour representation of the vertical deformation product from September 19, 2009 to December 24, 2009 superimposed on SAR image with 0.01 ft contours. . . . .	12
8	Zoom-in of Playa del Rey AOI. Colour representation of the summation of the vertical deformation products from June 15, 2009 to December 24, 2009 superimposed on SAR image with 0.01 ft contours. . . . .	14
9	Zoom-in of Playa del Rey Gas Storage Field. Colour representation of the summation of the vertical deformation products from June 15, 2009 to December 24, 2009 superimposed on SAR image with 0.01 ft contours. . . . .	15
10	Zoom-in of Playa del Rey Gas Storage Field. Colour representation of the summation of the vertical deformation products from June 15, 2009 to December 24, 2009 superimposed on SAR image without contours. . . . .	16
11	Zoom-in of area between Culver City, Ladera Heights and Windsor Hills. Colour representation of the summation of the vertical deformation products from June 15, 2009 to December 24, 2009 superimposed on SAR image without contours. . . . .	17





12	Zoom-in of Playa del Rey AOI. Colour representation of the summation of the vertical deformation products from June 15, 2009 to December 24, 2009 superimposed on SAR image without contours. .	18
13	Zoom-in of Playa del Rey AOI. Colour representation of the summation of the vertical deformation products from May 27, 2008 to December 24, 2009 superimposed on SAR image with 0.01 ft contours.	20
14	Zoom-in of Playa del Rey Gas Storage Field. Colour representation of the summation of the vertical deformation products from May 27, 2008 to December 24, 2009 superimposed on SAR image with 0.01 ft contours. . . . .	21
15	Zoom-in of Playa del Rey Gas Storage Field. Colour representation of the summation of the vertical deformation products from May 27, 2008 to December 24, 2009 superimposed on SAR image without contours. . . . .	22
16	Zoom-in of area between Culver City, Ladera Heights and Windsor Hills. Colour representation of the summation of the vertical deformation products from May 27, 2008 to December 24, 2009 superimposed on SAR image without contours. . . . .	23
17	Zoom-in of Playa del Rey AOI. Colour representation of the summation of the vertical deformation products from May 27, 2008 to December 24, 2009 superimposed on SAR image without contours. .	24
18	Zoom-in of area between Culver City, Ladera Heights and Windsor Hills. Colour representation of the summation of the vertical deformation products from May 27, 2008 to December 24, 2009 superimposed on SAR image without contours. . . . .	25
19	Definition of a 5.6-cm wave. . . . .	29
20	Electromagnetic spectrum. . . . .	30



## List of Tables

1	RADARSAT-2 Ultra-Fine data acquired over Playa del Rey Gas Storage Field . . . . .	3
2	Selected RADARSAT-2 data for the InSAR analysis . . . . .	3
3	Summary of Pair A . . . . .	4
4	Summary of Pair B . . . . .	4
5	Rainfall accumulation per month at the Los Angeles Airport (LAX). Source: National Weather Service. . . . .	5
6	Delivered Data . . . . .	27



## List of Acronyms



## 1 Interim Report B Objective

The objective of this report, Interim Report B, is to provide SoCalGas with measurements of the deformation that occurred within the project's AOI using conventional InSAR monitoring from June 2009 to December 2009. Nine (9) RADARSAT-2 Ultra-Fine ascending satellite data, acquired for this time period were examined. For this Milestone, two (2) conventional InSAR deformation maps quantifying movement are generated.

This deliverable pertains to the third deliverable, Milestone 3, of a five (5) year InSAR Monitoring Program, as described in Section 2.1 Table 1 Milestone Deliverables of the Master Document.

### 1.1 Report Organization

This report is organized as follows:

- Section 1 provides the introduction and report organization. This section also describes the AOI and the available data for the current monitoring time period.
- Section 2 describes the results for the two (2) deformation maps as well as the two (2) summation products.
- Section 3 provides a summary and conclusions.
- Appendix A lists the deliverables.
- Appendix B provides a list of definitions for commonly used terms.

### 1.2 Study Area

The Playa del Rey Gas Storage Field AOI and surrounding area, in Los Angeles, California, is outlined by the red polygon as seen in Figure 1. The corner coordinates for the polygon are approximately given by a rectangle with coordinates 34°01' 58"N 118°28' 5"W and 33°56' 56"N 118°20' 4"W.



Figure 1: Playa del Rey AOI and surrounding area in Los Angeles, as outlined by red polygon (radar amplitude image).



### 1.3 Data Selection

The RADARSAT-2 Ultra-Fine data used to generate the deliverables for the June 2009 to December 2009 time period are listed in Table 1 below.

Table 1: RADARSAT-2 Ultra-Fine data acquired over Playa del Rey Gas Storage Field

Acquisition #	Acquisition Date	Orbit Number	Comments
1	June 15, 2009	7839	Acquired
2	July 9, 2009	8182	Acquired
3	August 2, 2009	8525	Acquired
4	August 26, 2009	8868	Acquired
5	September 19, 2009	9211	Acquired
6	October 13, 2009	9554	Acquired
7	November 6, 2009	9897	Acquired
8	November 30, 2009	10240	Acquired
9	December 24, 2009	10583	Acquired

The two (2) InSAR deformation maps that were created are listed in Table 2. On these dates the SAR data were of best quality with suitable baselines. These two (2) maps are generated using the September 19, 2009 acquisition as the shared data, which allows for a comparison between them.

Table 2: Selected RADARSAT-2 data for the InSAR analysis. (The pairing numbers refer to the acquisition numbers from Table 1.)

Interferogram Pair	Acquisition Date Master	Acquisition Date Slave	Perpendicular Baseline (meters)
A (1-5)	Jun-15-09	Sept-19-09	-397
B (5-9)	Sept-19-09	Dec-24-09	-20

In addition, two (2) summation maps are generated. These provide an improvement in precision by summing the results of the two maps. Pair C is the summation from June 15, 2009 to September 19, 2009 and September 19, 2009 to December 24, 2009. Pair D is the summation from May 27, 2008 to December 24, 2009. For this product, the summation products delivered in the previous deliverables are added to the summation product of the current deliverable (Pair C). Masked areas for the overall summation are an accumulation of each of the previous masks.



## 2 Results - Interim Report B

Following the analysis of all available data, by evaluating all sequential combinations, two (2) interferometric pairs are selected for the generation of deformation products:

- Pair A for the time period between June 15, 2009 to September 19, 2009 (96 days)
- Pair B for the time period between September 19, 2009 to December 24, 2009 (96 days)

These data are selected because the generated interferograms are the best at these dates and are least affected by noise and the DEM error. A mask is applied in incoherent areas. The root-mean-square of the observed values in the deformation map is indicative of the precision of the deformation map. To obtain a 95% confidence interval a factor of two is used. Table 3 and Table 4 show the summary of the estimation of noise level for pairs A and B, respectively.

Table 3: Summary of Pair A

<b>Date</b>	<b>Time Span</b>	<b>Noise Level standard deviation [ft]</b>	<b>95% Confidence interval [ft]</b>
Jun-15-09 to Sept-19-09	96 days	0.0095	0.019

Table 4: Summary of Pair B

<b>Date</b>	<b>Time Span</b>	<b>Noise Level standard deviation [ft]</b>	<b>95% Confidence interval [ft]</b>
Sept-19-09 to Dec-24-09	96 days	0.0074	0.0148

The following sections present the results for both pairs A and B.

Additionally, summation products, Pair C and Pair D, have been created and are presented in this report.



## 2.1 Pair A - June 15, 2009 to September 19, 2009

The vertical deformation in the Playa del Rey Gas Storage Field is observed for the time period between June to September, 2009.

In order to extract reliable information from the generated deformation products, a low coherence mask is generated and applied to the deformation map. This mask is created by thresholding the coherence image. Coherence ( $\gamma$ ) values,  $\gamma < 0.17$ , are considered areas of low coherence and are masked out with values set to -999.

Deformation is observed in the Playa del Rey Gas Storage Field AOI, as can be seen from the vertical deformation product shown in Figure 3. This deformation could be attributed to lack of rainfall. As shown in Table 5, historical weather data for the Los Angeles airport, rainfall amounts from June to September could be attributed to subsidence in the Playa del Rey Gas Storage Field.

A color representation is shown in Figure 4 and Figure 2 of the final product after masking areas that contain noise. The estimated precision for Pair A is within  $\pm 0.019$  ft with a 95% confidence interval.

Table 5: Rainfall accumulation per month at the Los Angeles Airport (LAX). Source: National Weather Service.

Month	Monthly Precipitation [inches]
June 2009	0.15
July 2009	0.00
August 2009	0.00
September 2009	Trace
October 2009	1.31
November 2009	0.00
December 2009	2.05

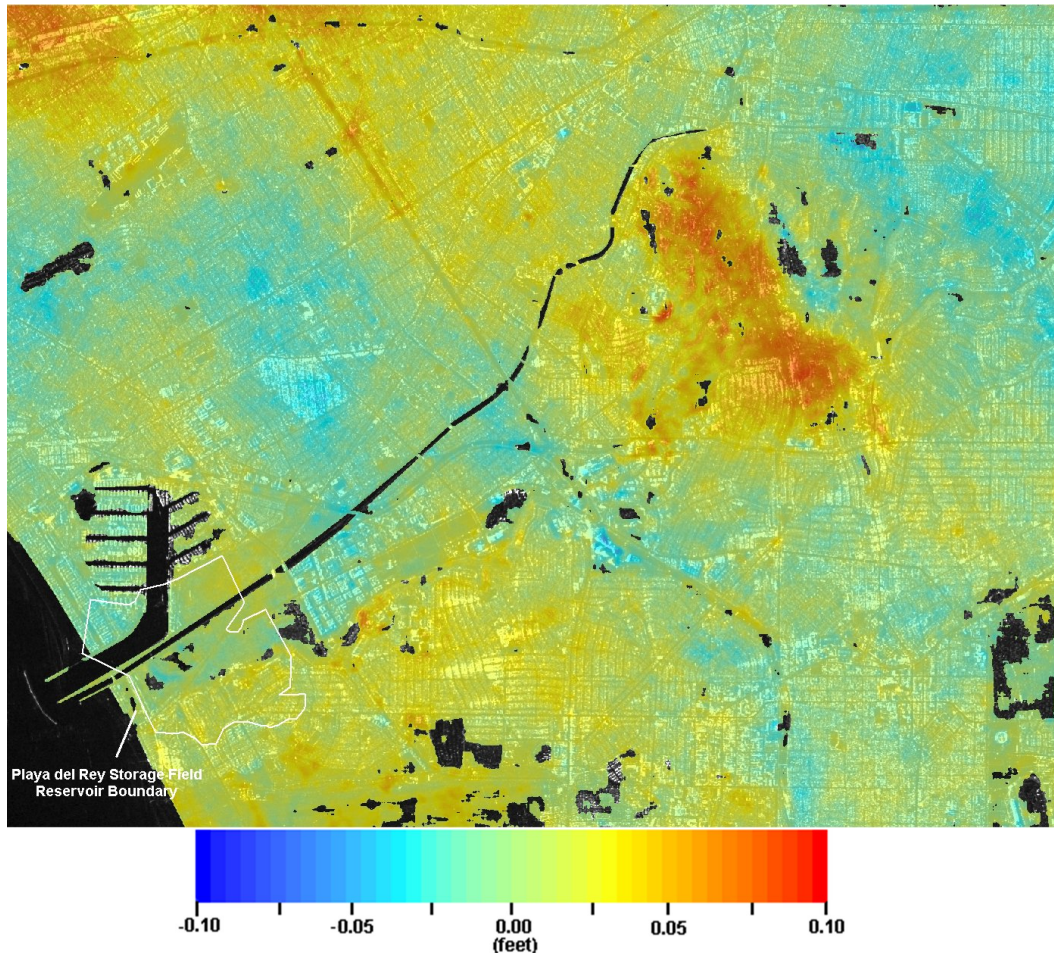


Figure 2: Zoom-in of Playa del Rey AOI. Colour representation of the vertical deformation product from June 15, 2009 to September 19, 2009 superimposed on SAR image without contours. In this representation, blue corresponds to subsidence and red indicates uplift.

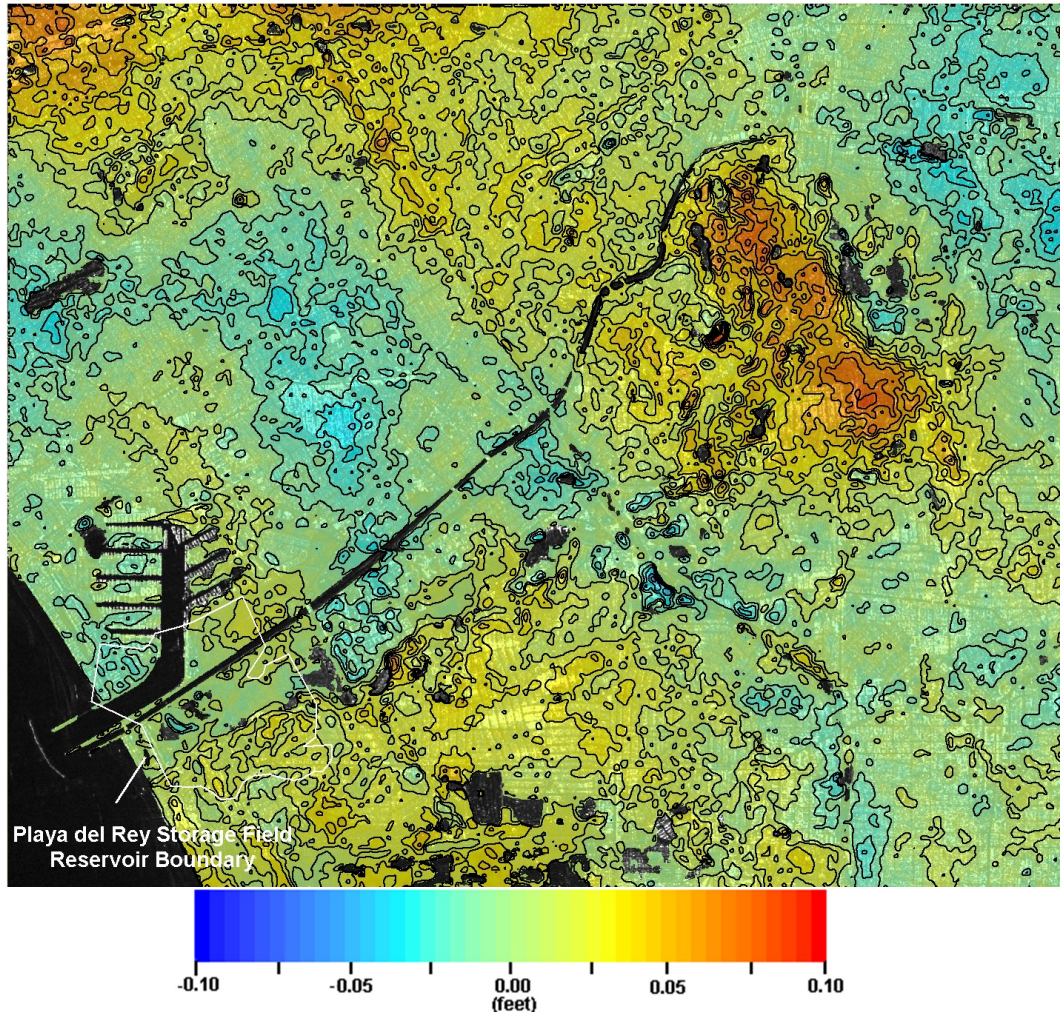


Figure 3: Zoom-in of Playa del Rey AOI. Colour representation of the vertical deformation product from June 15, 2009 to September 19, 2009 superimposed on SAR image with 0.01 ft contours. In this representation, blue corresponds to subsidence and red indicates uplift.

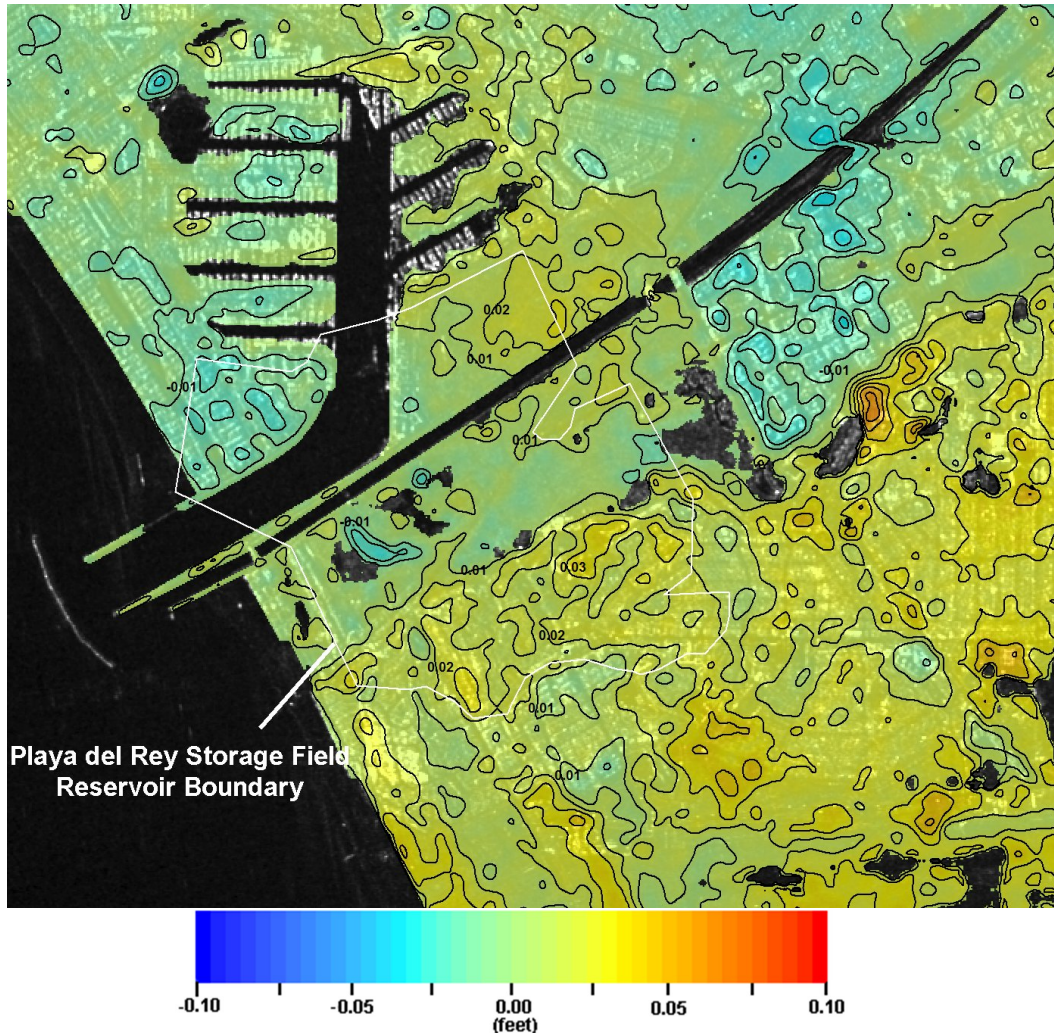


Figure 4: Zoom-in of Playa del Rey Gas Storage Field. Colour representation of the vertical deformation product from June 15, 2009 to September 19, 2009 superimposed on SAR image with 0.01 ft contours. In this representation, blue corresponds to subsidence and red indicates uplift.

## 2.2 Pair B - September 19, 2009 to December 24, 2009

The deformation in the Playa del Rey Gas Storage Field is observed for the time period between September to December, 2009.

In order to extract reliable information from the generated deformation products, a low coherence mask is generated and applied to the deformation map. This mask is created by thresholding the coherence image. Coherence ( $\gamma$ ) values,  $\gamma < 0.17$ , are considered areas of low coherence and are masked out with values set to -999.

Uplift is observed in the Playa del Rey Gas Storage Field AOI, as can be seen from the vertical deformation product shown in Figure 6. This uplift can be attributed to surface moisture due to rainfall from period September to December, as shown in Table 5, historical weather data for the Los Angeles airport.

Figure 7 and Figure 5 present a color representation of the final product after masking areas that contain noise. The estimated precision for Pair B is within  $\pm 0.0148$  ft with a 95% confidence interval.

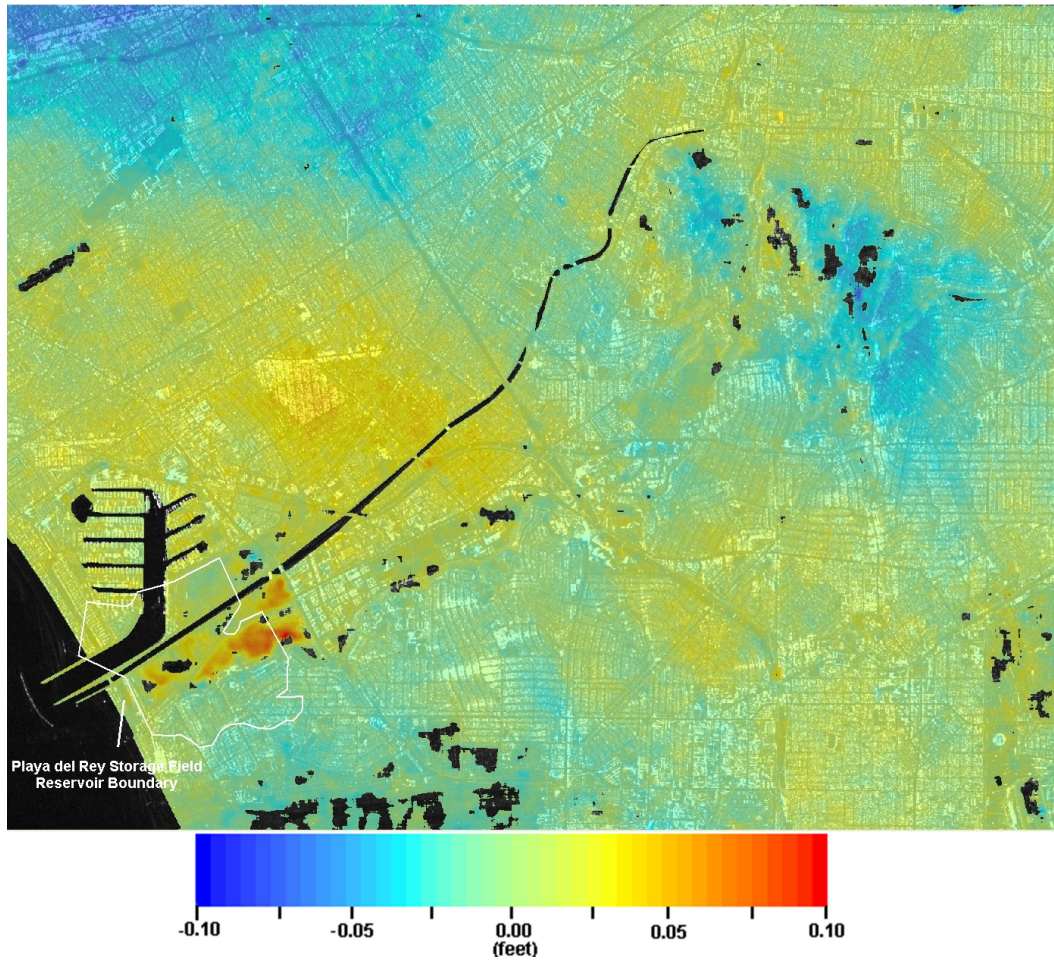


Figure 5: Zoom-in of Playa del Rey AOI. Colour representation of the vertical deformation product from September 19, 2009 to December 24, 2009 superimposed on SAR image without contours. In this representation, blue corresponds to subsidence and red indicates uplift.

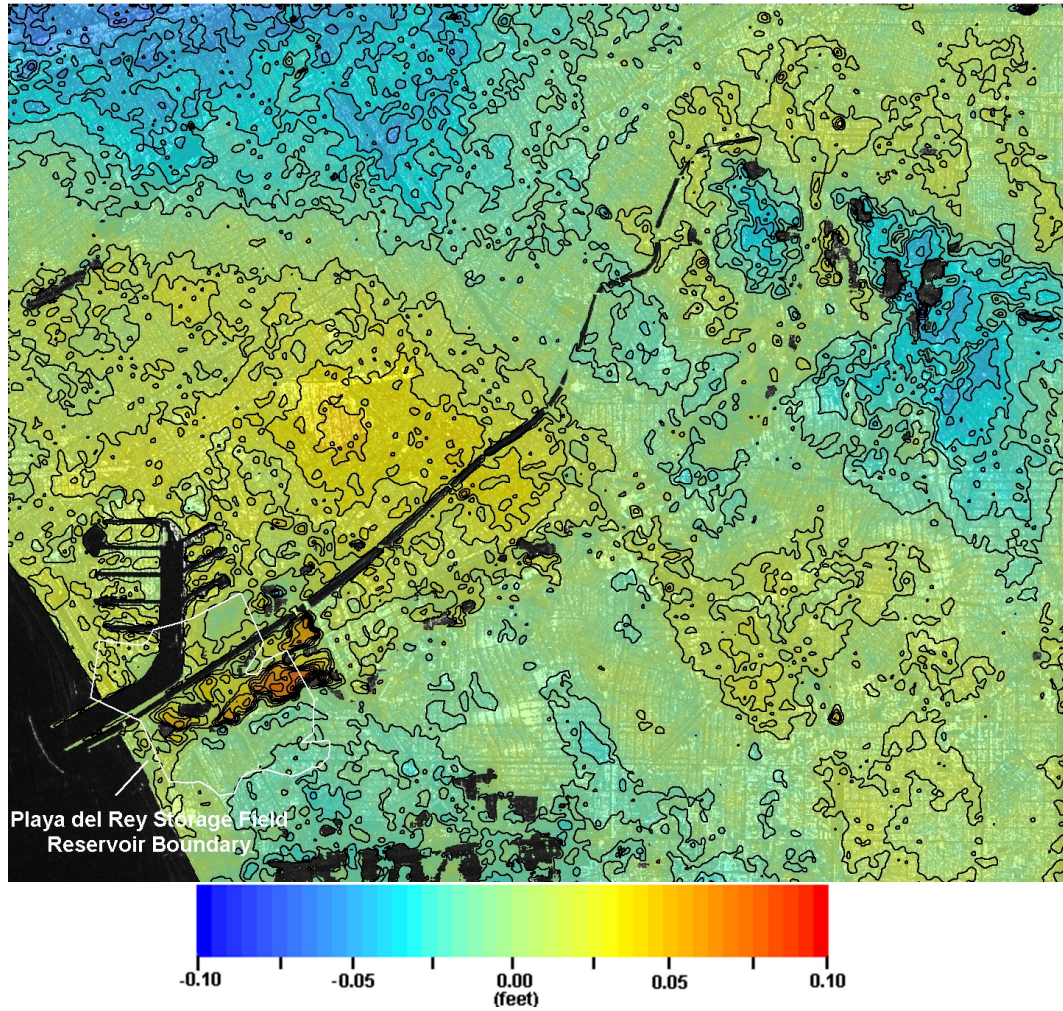


Figure 6: Zoom-in of Playa del Rey AOI. Colour representation of the vertical deformation product from September 19, 2009 to December 24, 2009 superimposed on SAR image with 0.01 ft contours. In this representation, blue corresponds to subsidence and red indicates uplift.

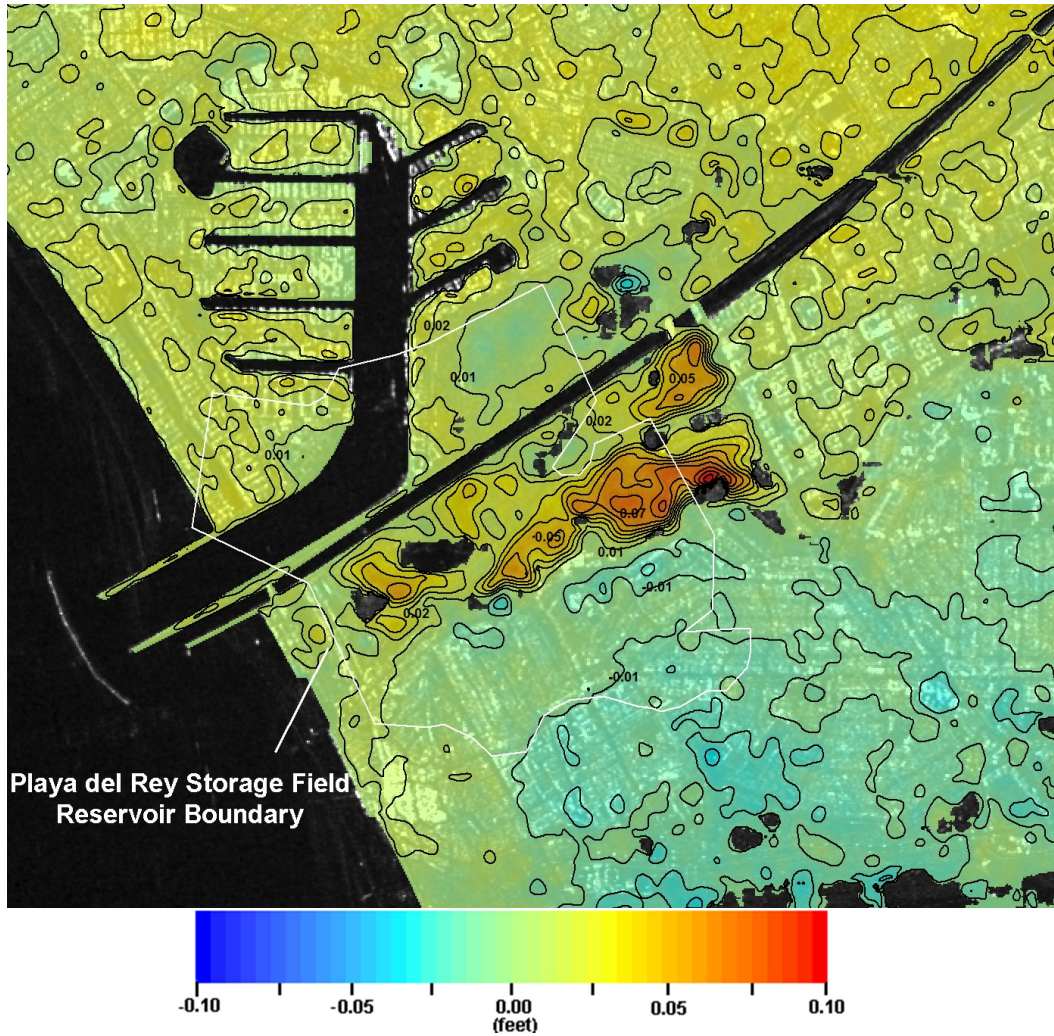


Figure 7: Zoom-in of Playa del Rey Gas Storage Field. Colour representation of the vertical deformation product from September 19, 2009 to December 24, 2009 superimposed on SAR image with 0.01 ft contours. In this representation, blue corresponds to subsidence and red indicates uplift.



### **2.3 Pair C - Summation June 15, 2009 to December 24, 2009**

Figure 8 shows the summation of the individually estimated deformation results during the two (2) time periods (June 2009 to September 2009 and September 2009 to December 2009). This is a better estimate of the actual deformation that occurred in this time frame because independent noise in the two individual deformation maps is summed.

In particular, atmospheric effects that contribute to noise are independent in the two maps and minimized by taking the average. From Figure 8, Figure 9 and Figure 10, the averaged colour representation of the maps, there is a relatively small amount of deformation occurring in the Playa del Rey Gas Storage Field AOI, which could be attributed to natural terrain expansion, i.e., moisture in the ground.

Subsidence is observed however over an area situated between Windsor Hills and Ladera Heights, center coordinate 34°00' 17"N 118°21'21"W. Subsidence in this area is in the order of 0.03 - 0.05 ft as shown in Figure 11 to Figure 12. West of the subsidence is an area of uplift, center coordinate 34°00' 11"N 118°22' 35"W. Uplift in this area is in the order of 0.03 - 0.09 ft as shown in Figure 11 to Figure 12.

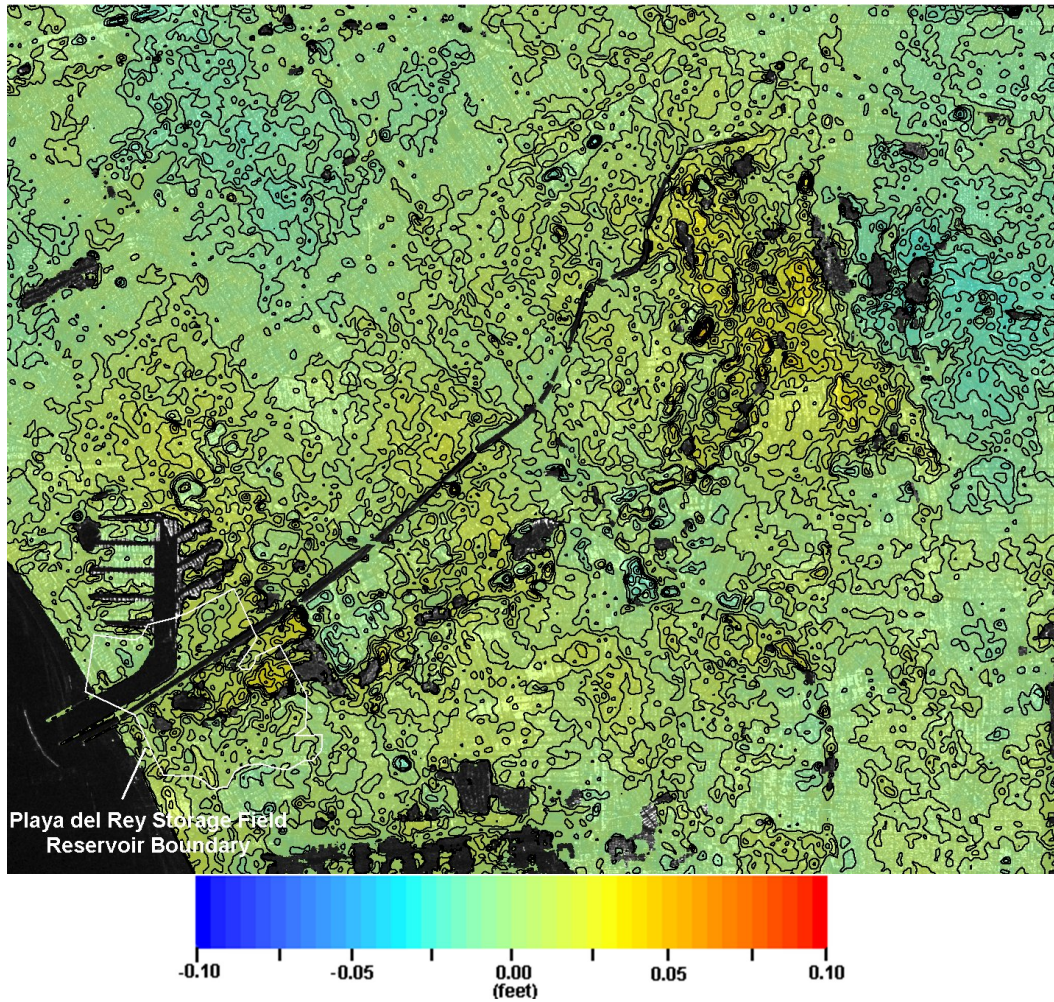


Figure 8: Zoom-in of Playa del Rey AOI. Colour representation of the summation of the vertical deformation products from June 15, 2009 to December 24, 2009 superimposed on SAR image with 0.01 ft contours. In this representation, blue corresponds to subsidence and red indicates uplift.

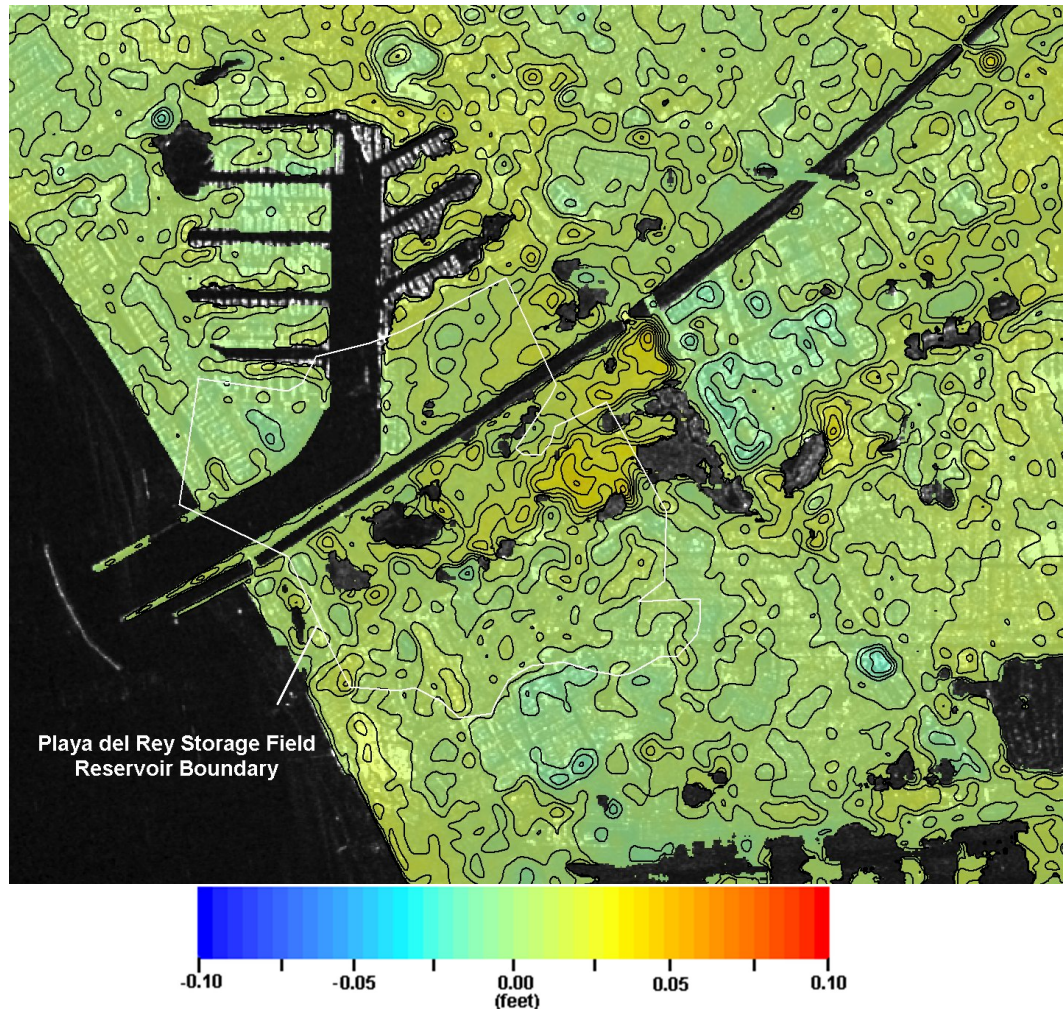


Figure 9: Zoom-in of Playa del Rey Gas Storage Field. Colour representation of the summation of the vertical deformation products from June 15, 2009 to December 24, 2009 superimposed on SAR image with 0.01 ft contours. In this representation, blue corresponds to subsidence and red indicates uplift.

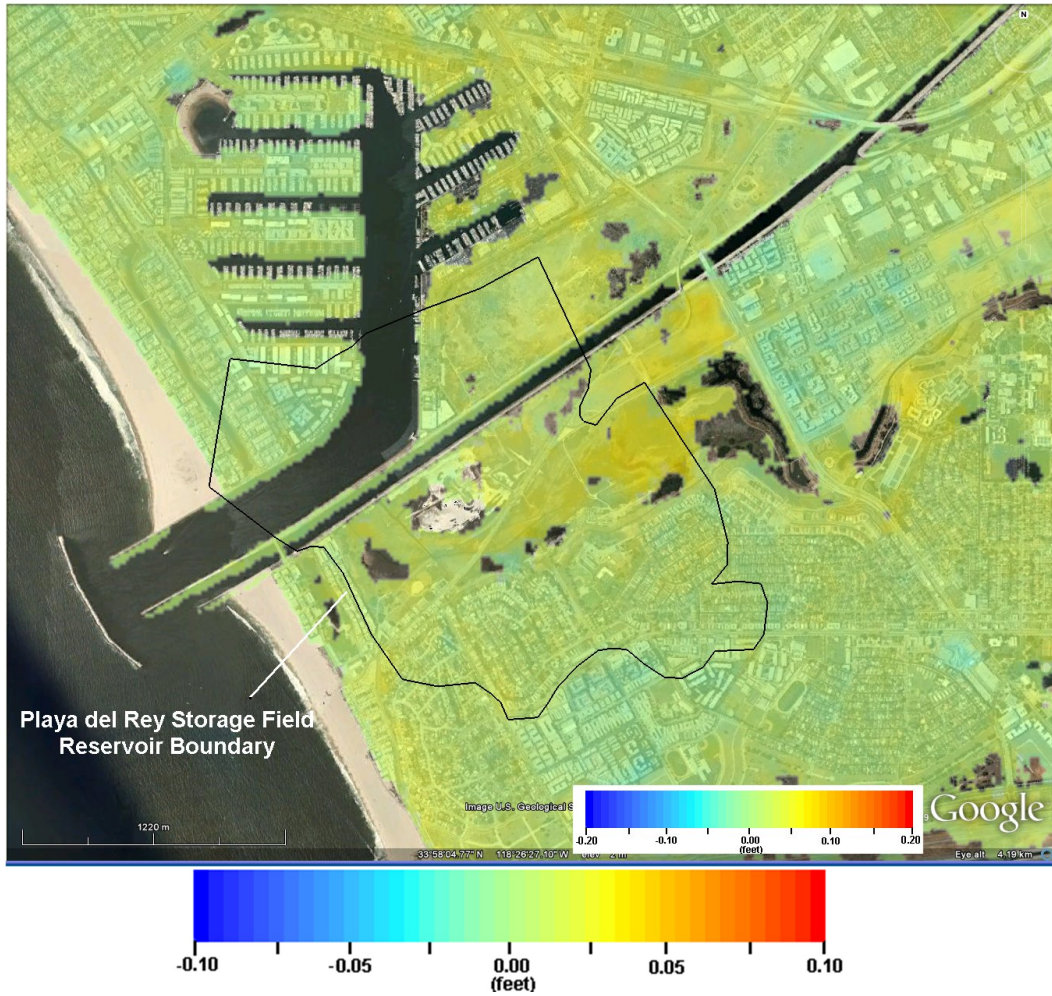


Figure 10: Zoom-in of Playa del Rey Gas Storage Field. Colour representation of the summation of the vertical deformation products from June 15, 2009 to December 24, 2009 superimposed on SAR image without contours. In this representation, blue corresponds to subsidence and red indicates uplift.

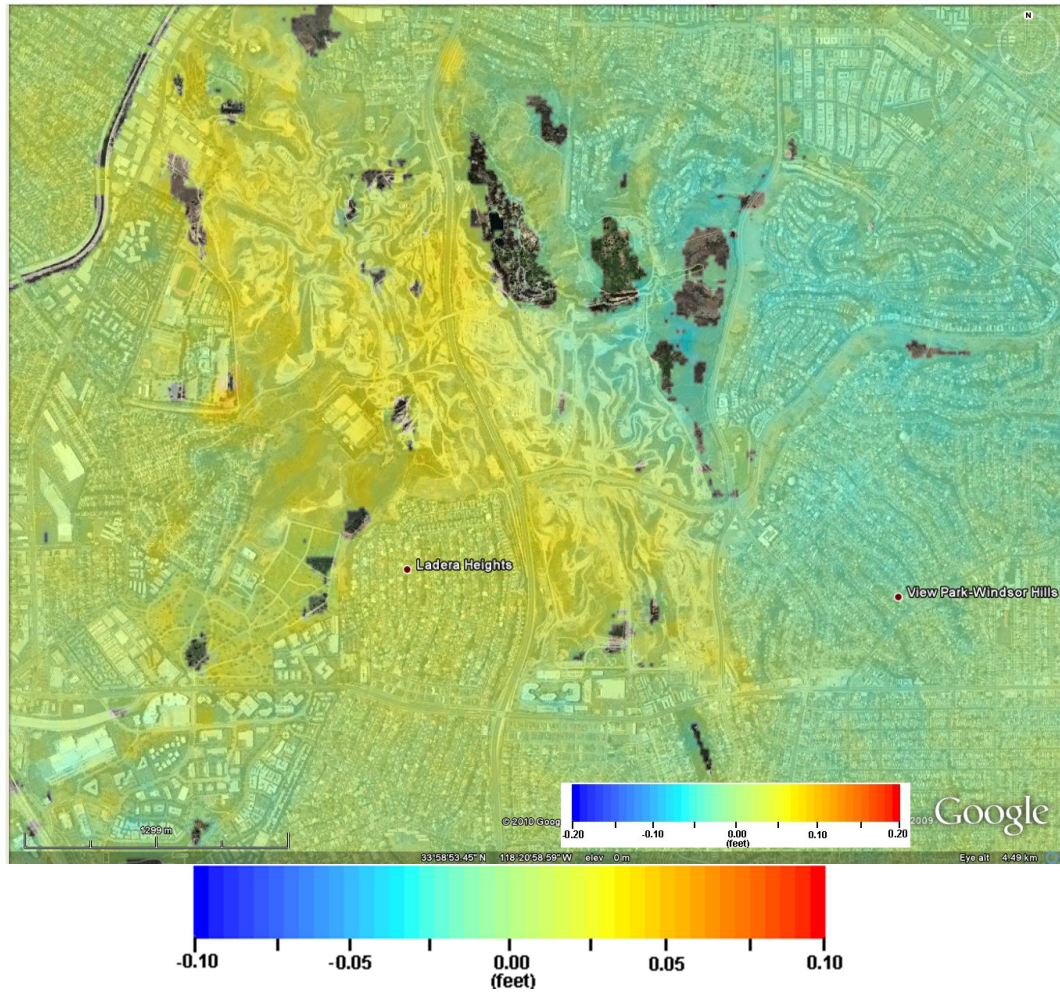


Figure 11: Zoom-in of area between Culver City, Ladera Heights and Windsor Hills. Colour representation of the summation of the vertical deformation products from June 15, 2009 to December 24, 2009 superimposed on SAR image without contours. In this representation, blue corresponds to subsidence and red indicates uplift.

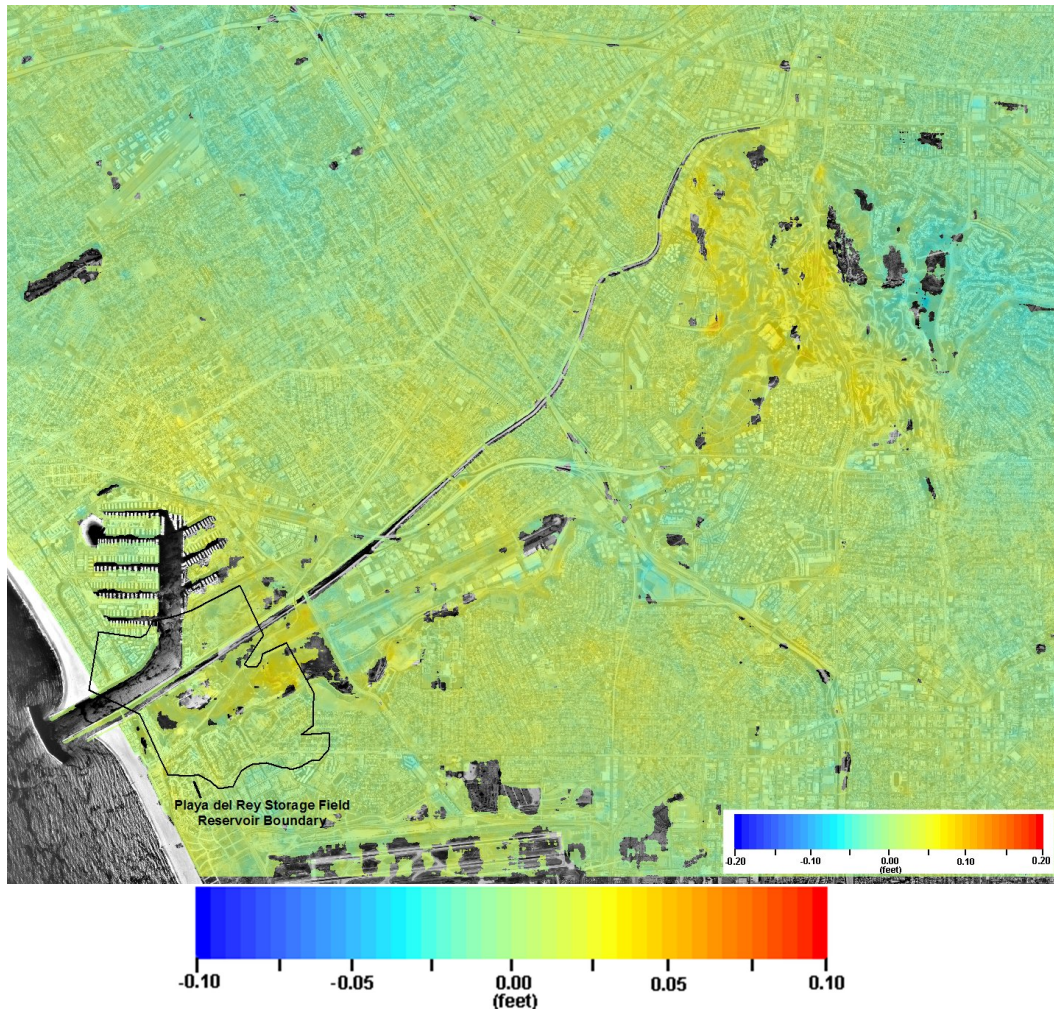


Figure 12: Zoom-in of Playa del Rey AOI. Colour representation of the summation of the vertical deformation products from June 15, 2009 to December 24, 2009 superimposed on SAR image without contours. In this representation, blue corresponds to subsidence and red indicates uplift.

## **2.4 Pair D - Summation May 27, 2008 to December 24, 2009**

Figure 13 shows the summation of the individually estimated deformation results starting May 27, 2008 (May 2008 to August 2008, August 2008 to December 2008, December 2008 to March 2009, March 2009 to June 2009, June 2009 to September 2009, September 2009 to December 2009). From Figure 13, Figure 14 and Figure 15, the averaged colour representation of the maps, there is deformation occurring in the Playa del Rey Gas Storage Field AOI. This result could be attributed to natural terrain expansion related to the relatively high precipitation during this time period (June 2009 to September 2009).

Subsidence is observed over an area situated between Ladera Heights and Windsor Hills, center coordinate 33°59' 38"N 118°21' 51"W. Subsidence in this area is in the order of 0.05 - 0.13 ft as shown in Figure 16 and Figure 18. Uplift is observed over an area situated between Ladera Heights and Culver City, center coordinate 34°0' 37"N 118°23' 06"W. Uplift in this area is in the order of 0.05 - 0.12 ft as shown in Figure 16 and Figure 18.

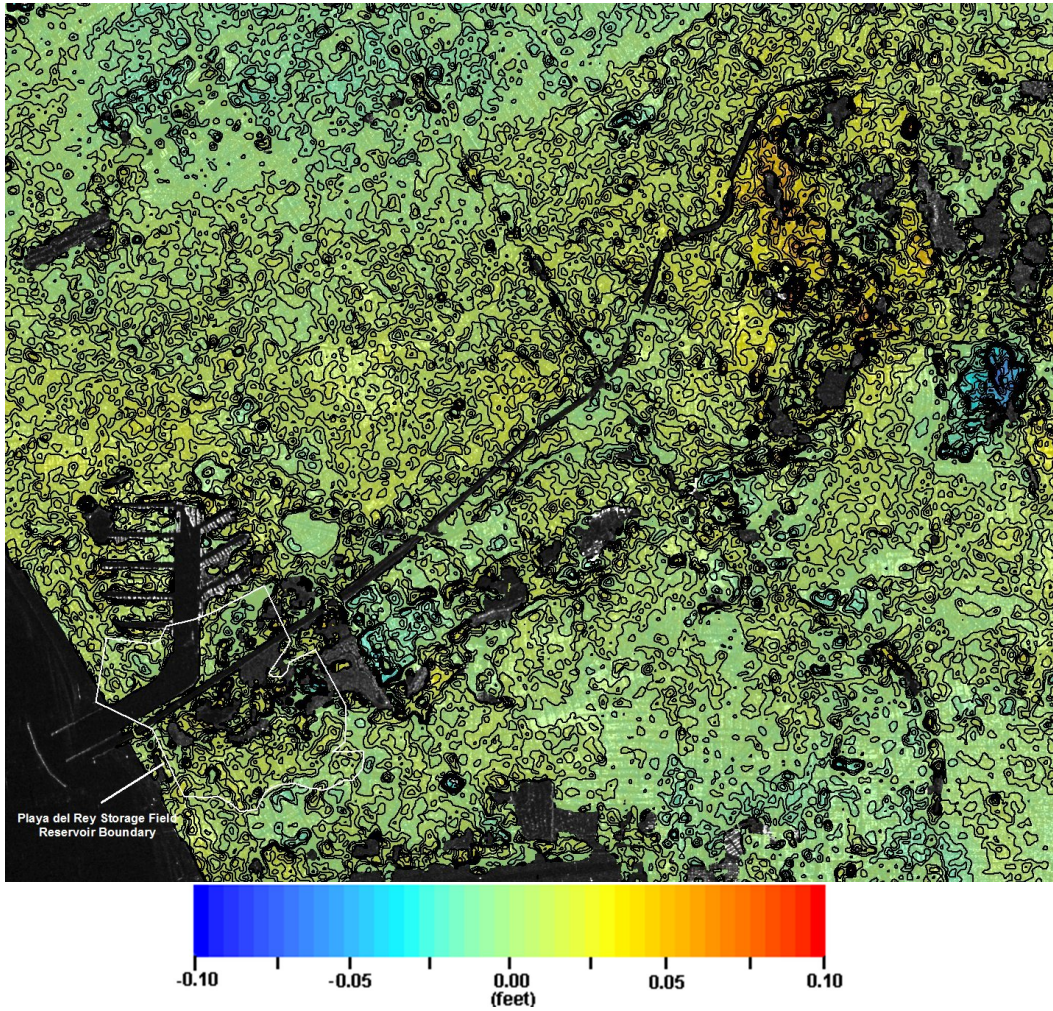


Figure 13: Zoom-in of Playa del Rey AOI. Colour representation of the summation of the vertical deformation products from May 27, 2008 to December 24, 2009 superimposed on SAR image with 0.01 ft contours. In this representation, blue corresponds to subsidence and red indicates uplift.



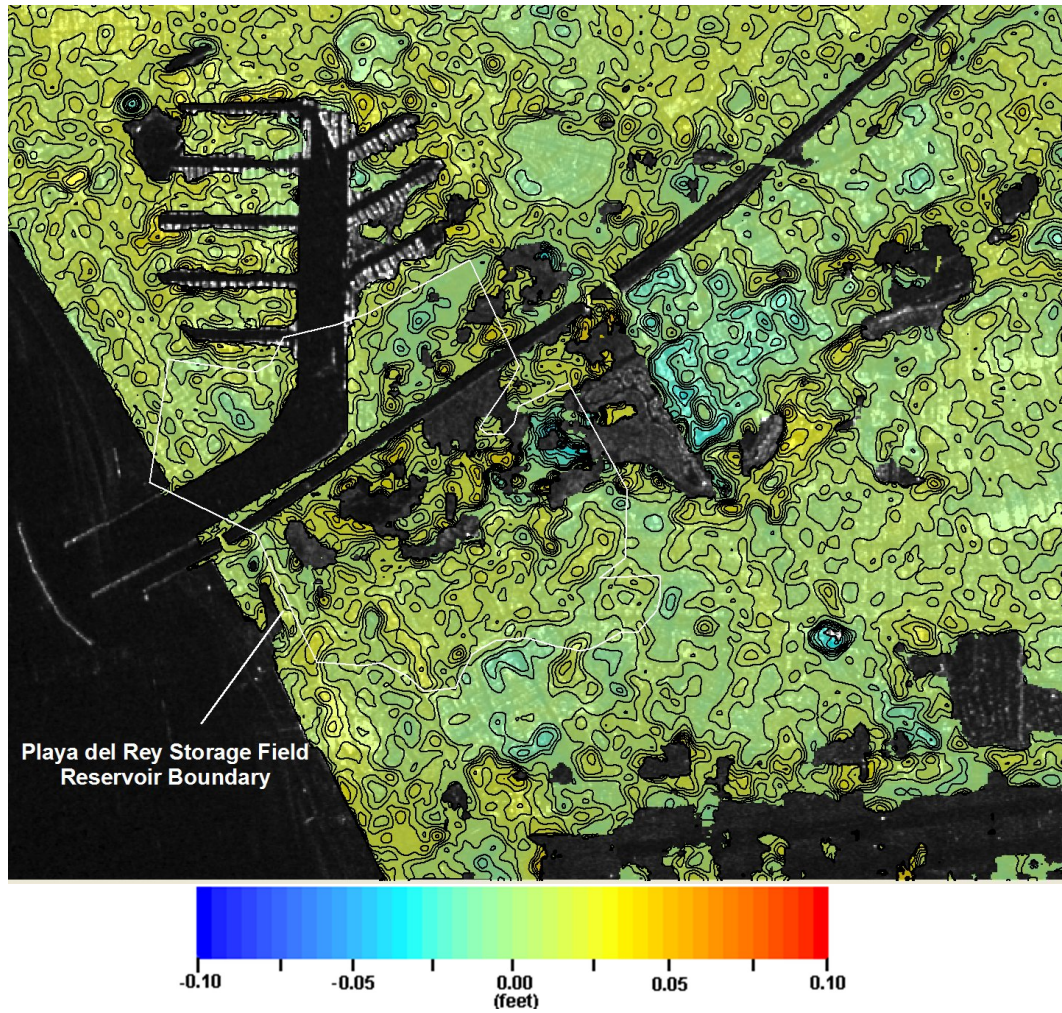


Figure 14: Zoom-in of Playa del Rey Gas Storage Field. Colour representation of the summation of the vertical deformation products from May 27, 2008 to December 24, 2009 superimposed on SAR image with 0.01 ft contours. In this representation, blue corresponds to subsidence and red indicates uplift.

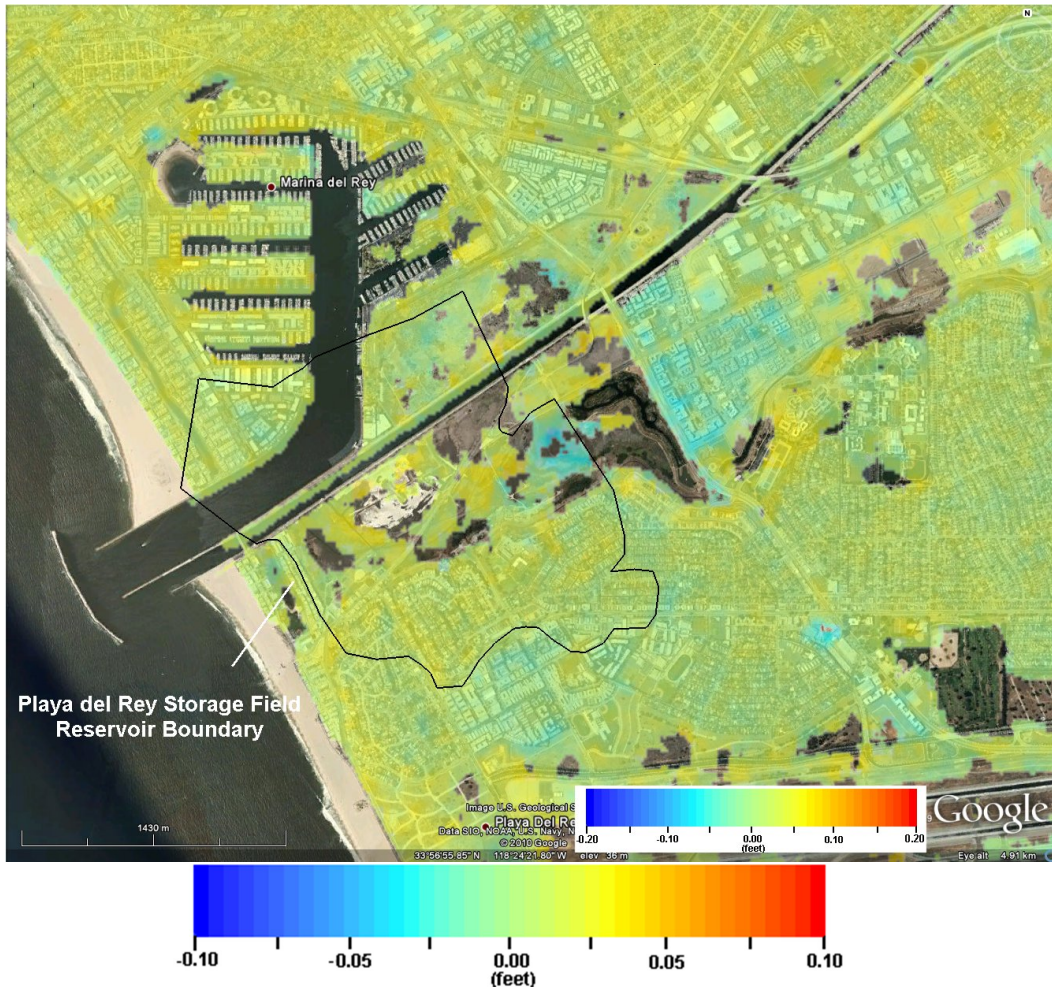


Figure 15: Zoom-in of Playa del Rey Gas Storage Field. Colour representation of the summation of the vertical deformation products from May 27, 2008 to December 24, 2009 superimposed on SAR image without contours. In this representation, blue corresponds to subsidence and red indicates uplift.

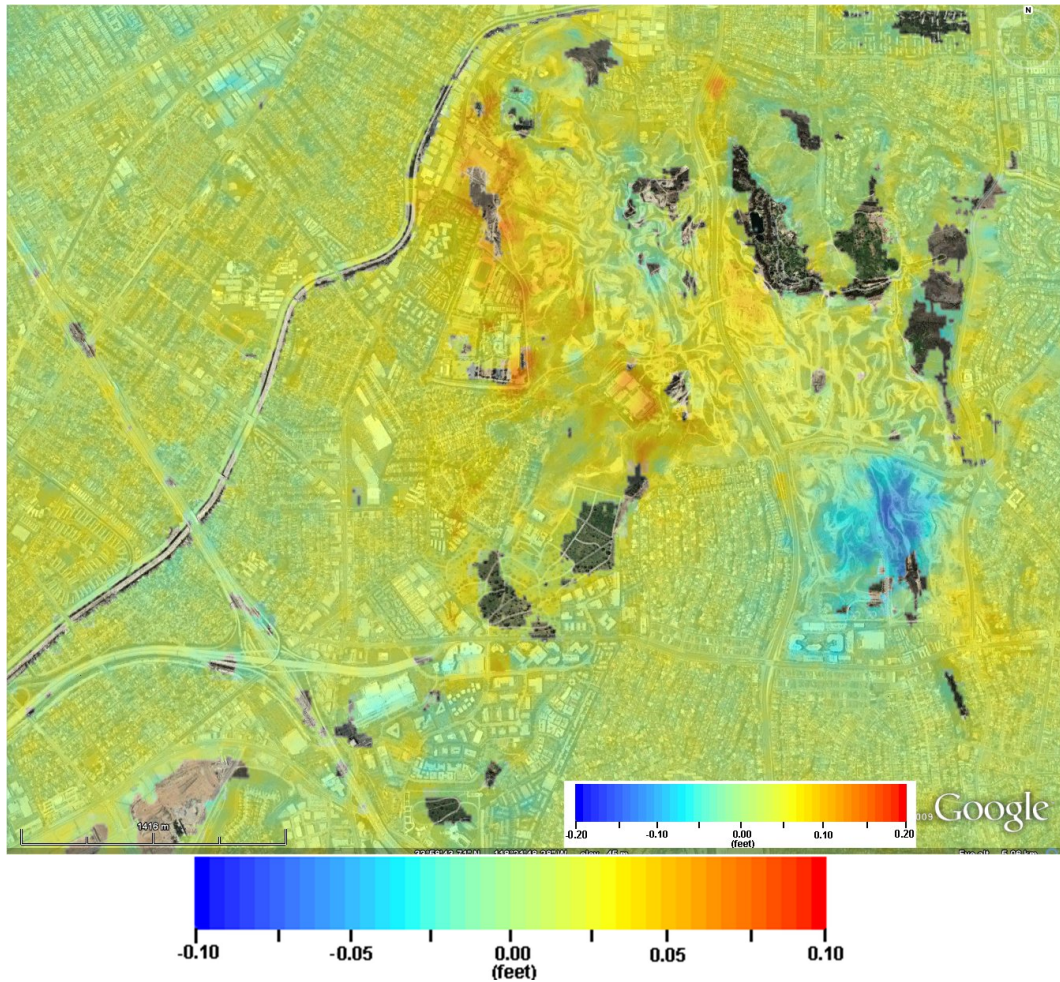


Figure 16: Zoom-in of area between Culver City, Ladera Heights and Windsor Hills. Colour representation of the summation of the vertical deformation products from May 27, 2008 to December 24, 2009 superimposed on SAR image without contours. In this representation, blue corresponds to subsidence and red indicates uplift.

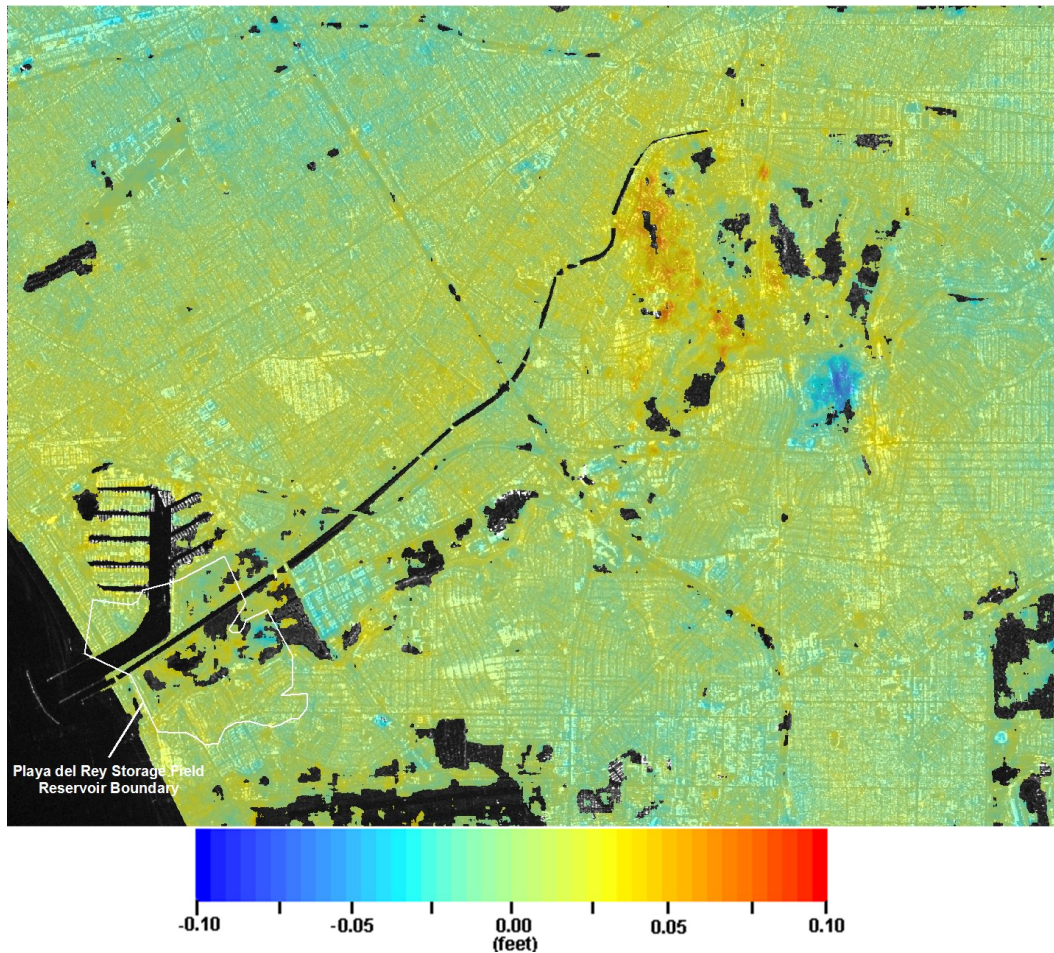


Figure 17: Zoom-in of Playa del Rey AOI. Colour representation of the summation of the vertical deformation products from May 27, 2008 to December 24, 2009 superimposed on SAR image without contours. In this representation, blue corresponds to subsidence and red indicates uplift.

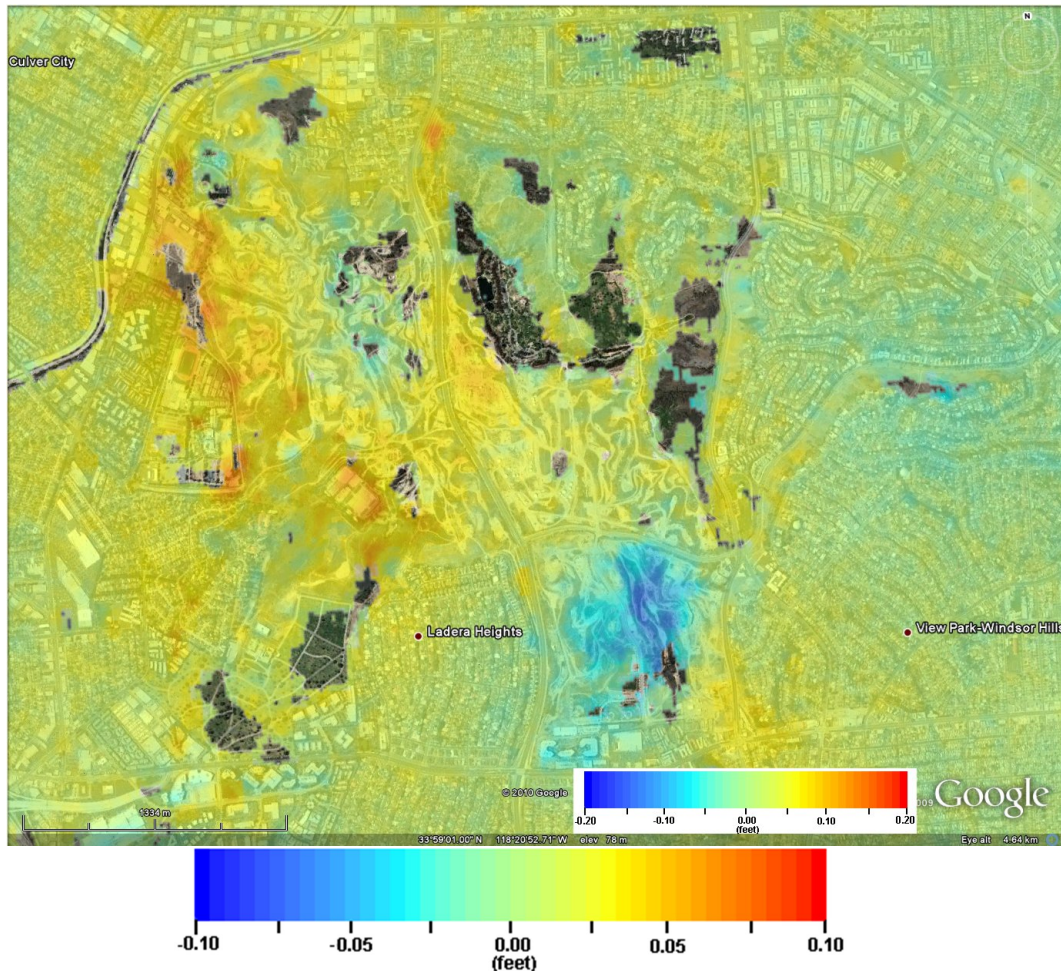


Figure 18: Zoom-in of area between Culver City, Ladera Heights and Windsor Hills. Colour representation of the summation of the vertical deformation products from May 27, 2008 to December 24, 2009 superimposed on SAR image without contours. In this representation, blue corresponds to subsidence and red indicates uplift.



### 3 Concluding Remarks

Vertical surface deformation measurements are calculated for the Playa del Rey Gas Storage Field and surrounding areas in Los Angeles using conventional radar interferometry (InSAR). This report, referred to as Interim Report B, pertains to Milestone 3 of the current contract.

The following items describe the main findings of the work performed, as per Milestone 2:

- RADARSAT-2 Ultra-Fine ascending data were scheduled by MDA for acquisition. The acquired data, covering the period of June 2009 to December 2009, were analyzed and utilized as part of the deliverables.
- Two (2) deformation maps were generated as part of the third Milestone of a five (5) year monitoring program.
- Deformation and uplift can be attributed to surface moisture in the area of interest. During the time period from June 2009 to September 2009, minimal rainfall occurred resulting in a decrease in natural terrain moisture. Subsequently rainfall accumulation contributed to natural terrain expansion, hence uplift from period September to December 2009.
- The estimated precision for the Pair A vertical deformation product is 0.019 ft with a 95% confidence interval; while the estimated precision for Pair B vertical deformation product is 0.0148 ft with a 95% confidence interval.
- Two (2) summation products are generated. The first is for the six (6) month time period from June 15, 2009 to December 24, 2009 (Pair C). For this period, masked areas are interpolated and common mask areas between the two individual vertical deformation products are extracted and applied to the final summation product.
- The second summation product includes approximately one and a half (1.5) years of monitoring from May 27, 2008 to December 24, 2009 (Pair D). This was derived by combining the previous and current time period summation products. Mask areas for this overall summation is an accumulation of all the previous masks.



## A Deliverables

The deliverables, which are included on CD-ROM for Milestone 3, are listed in Table 6. These delivered data are described in XYZ ASCII files and are in California US State Plane, NAD27, 65.62 ft spacing.

Table 6: Delivered Data

<b>Deliverable file</b>	<b>Description</b>
PlayadelRey_SoCalGas_InterimReportB_2010.pdf	Interim Report B in PDF format.
<b>Conventional Deformation map</b>	
061509_091909_DEF.xyz 061509_091909_DEF.tif  091909_122409_DEF.xyz 091909_122409_DEF.tif  SUM_061509_122409_DEF.xyz SUM_061509_122409_DEF.tif  SUM_052708_122409_DEF.xyz SUM_052708_122409_DEF.tif	ASCII files with location and vertical deformation measurements in ft. Coherence ( $\gamma$ ) values, $\gamma < 0.17$ , are considered areas of low coherence and are masked out with values set to -999.  Additional format supplied as Geotiff.
Projection_Report.pdf	Describes the coordinate projection system of the delivered data.

## B Standard Definitions

**Amplitude ( $a$ )** The amplitude of a wave is the distance from the centre of the wave to the peak, see Figure 19.

**Ascending** Satellite tracks that transit from the south to the north are labeled ascending.

**Aspect Angle ( $\alpha$ )** The aspect angle is the angle at which the local area is observed.

**Azimuth** Azimuth or track describes the direction of travel of the sensor over the ground.

**Baseline ( $B$ )** The baseline is the vector describing the distance between two radar observations of the same point (see also perpendicular baseline).

**Coherence ( $\gamma$ )** Coherence,  $\gamma$ , is used as a measure of the degree of similarity between the backscatter (amplitude and phase) response of coregistered SAR returns over time or space.

**Coregistration** Coregistration is the process of locating subsequent radar images to the same observation space. A set of coregistered images show information from the same point on the ground at the same image coordinate.

**Descending** Satellite tracks that transit from the north to the south are labeled descending.

**Electromagnetic Wave** An electromagnetic wave is a self-propagating wave that may exist in a vacuum or in matter. The wave has both electric and magnetic field components that oscillate with perpendicular phase. Electromagnetic radiation exists on a spectrum from gamma-rays to long radio waves. The visible spectrum is narrowly between 400 and 700 nm. Microwaves, the radiation used in SAR observations, are generally between a fraction of a millimetre and a metre in length.

**Frequency ( $f$ )** Frequency describes the number of cycles per second. Frequency is given in Hertz (Hz). For an electromagnetic wave, wavelength,  $\lambda$ , and frequency,  $f$ , are related through the speed of light,  $c$ , as  $c = \lambda f$ .

**Frequency Band** Radar frequencies are often referred to by a band letter. The coding goes back to the research conducted during WWII. C-Band extends from approximately 4-8 GHz. RADARSAT-1 & 2, ENVISAT, and ERS-1 & 2 all operate in C-Band. L-Band at 1-2 GHz was the operating frequency of



the original SEASAT satellite in the 1970s, and the ALOS satellite currently operates in that range. The TerraSAR-X satellite operates in X-Band (8-12 GHz). Figure 20 shows the electromagnetic spectrum.

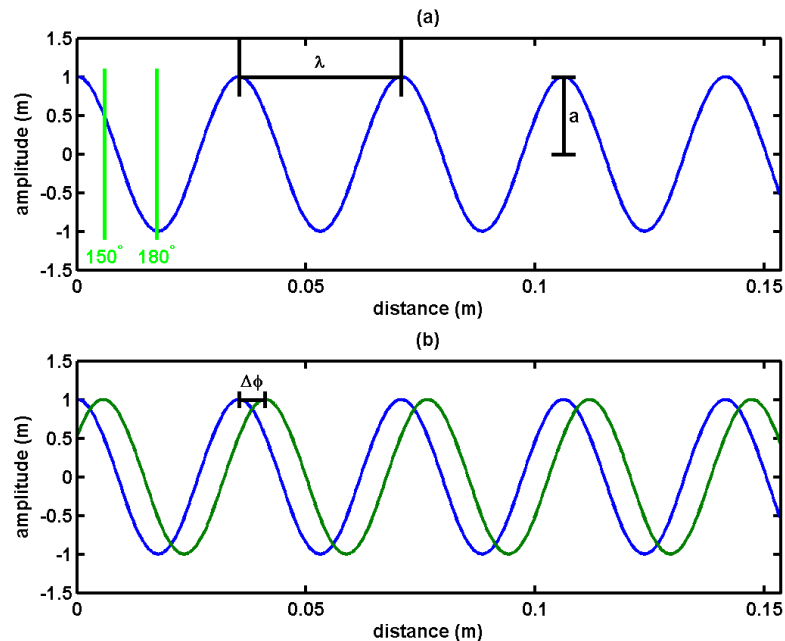


Figure 19: Definition of a 5.6-cm wave. Panel (a) shows the definition of wavelength,  $\lambda$ , and amplitude ( $a$ ). The green lines show the location on the wave associated with  $150^\circ$  and  $180^\circ$  of phase. Panel (b) demonstrates the phase difference,  $\Delta\phi$ , between two waves.

**Georeferencing** Georeferencing is the procedure used to assign individual radar observations to geographic positions. The process involves calculating the geographic position based on the time to target and the observation time of the radar. Georeferencing for RADARSAT-2 has been measured (based only on the state vectors and the imaging geometry) to be better than 20 m on the ground.

**Incident Angle ( $\theta_i$ )** The incident angle is the angle the incident radiation makes with respect to the surface normal. In satellite remote sensing,  $\theta_i$  is often used to describe the angle between the mean surface normal and the incident radiation.

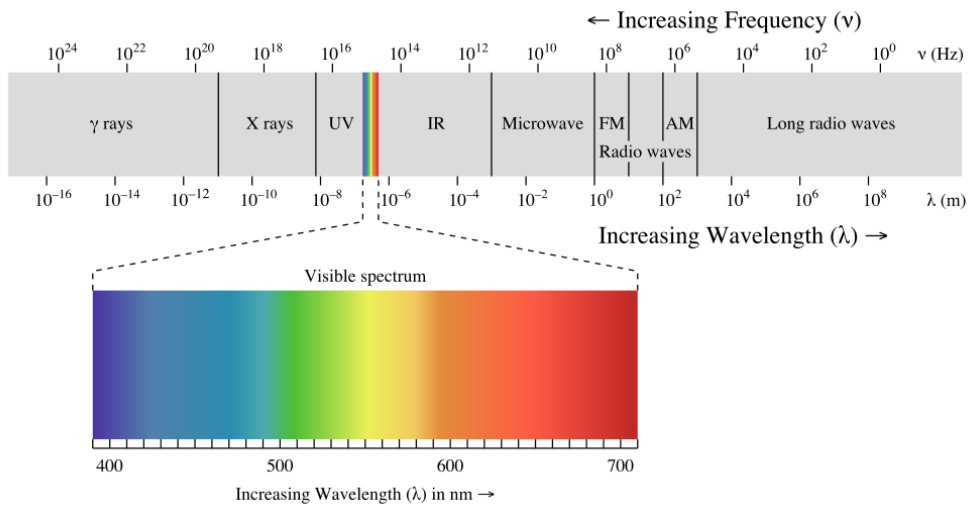


Figure 20: Electromagnetic spectrum showing the wavelength and frequency characteristics of radiation. The microwave portion of the spectrum contains the waves used for RADAR observation.

**Line of Sight** The line of sight describes travel of a wave from the radar to a point on the ground. Observations are only possible along the line of sight.

**Look Direction** Look direction refers to the side of the radar track (or azimuth) that the antenna pattern illuminates. That is, a right looking radar sends energy at approximately  $90^\circ$  to the right of the azimuth track.

**Pass** Pass or pass direction is used to refer to an ascending or descending satellite azimuth.

**Perpendicular Baseline** ( $B_{perp}$  or  $B_{\perp}$ ) is the separation of two radar observations in the direction perpendicular to the first radar observation.

**Phase** ( $\phi$ ) Phase describes the position on a wave. Figure 19 shows a wave with phase labeled as  $150^\circ$  and  $180^\circ$ .  $\phi$  is often reported in radians from 0 to  $2\pi$ , which corresponds to degrees from 0 to 360.

**Phase Difference** ( $\Delta\phi$ ) The phase difference (or phase shift) describes the difference between the position on two waves. Figure 19 shows a phase difference of  $60^\circ$  or  $\pi/3$ . The accuracy with which the phase difference can be measured is why InSAR is so valuable.

**Phase Noise** Phase noise refers to artifacts present in the phase measurement that are not due to the signal we want to capture.

**Range ( $\rho$  or  $R_i$ )** Range is used to describe the distance between a radar target on the ground and the sensor.

**Slant Range** Native SAR observations are recorded by time to target and time of observation. Slant range describes the distance along the radar line of sight.

**Slant Range Coordinates** The coordinate system of the native radar observations, defined by time of observation (azimuth) and time to target (slant range). Observations are aligned as range and azimuth pixels with constant spacing in slant range and slow time.

**Speed of Light ( $c$ )** The speed of light is 299 792 458 m/s.

**Temporal Decorrelation** As the time between observations increases, the physical reasons for the similarity of observations may change. In the monitoring of a field, for instance, the growth of grasses over time will cause decorrelation of the backscatter.

**Wavelength ( $\lambda$ )** Wavelength describes the distance between subsequent points of equal phase in consecutive cycles of a wave.